2162-8769/2018/7(6)/R99/5/$37.00 © The Electrochemical Society

High-Efficiency and High-Luminance Three-Color White Organic Light-Emitting Diodes with Low Efficiency Roll-Off

Junhong Zhou,[1] Jianhua Zou,[2] Caihong Dai,[3] Yong Zhang,[1] Xudong Luo,[1,z] and Baiquan Liu [2,4,z]

[1]*Guangdong Provincial Institute of Metrology, Key Laboratory of Geometric and Mechanical Measurement Technology in Guangdong Province, National Intelligent Control System Manufacturing Industry Centre of Metrology, Guangzhou 510405, People's Republic of China*
[2]*Institute of Polymer Optoelectronic Materials and Devices, State Key Laboratory of Luminescent Materials and Devices, South China University of Technology, Guangzhou 510640, People's Republic of China*
[3]*National Institute of Metrology, Beijing 100029, People's Republic of China*
[4]*LUMINOUS! Center of Excellence for Semiconductor Lighting and Displays, School of Electrical and Electronic Engineering, Nanyang Technological University, 639798, Singapore*

For the first time, double blue emitting layers have been functioned as the main exciton generation zone to achieve high-performance three-color phosphorescent white organic light-emitting diodes (WOLEDs). The WOLED exhibits the maximum forward-viewing external quantum efficiency (EQE) and power efficiency (PE) of 21.2% and 50.0 lm/W, respectively. Even at 1000 cd/m^2, the forward-viewing EQE and PE are as high as 18.0% and 32.5 lm/W, respectively, indicating low efficiency roll-off. Besides, the WOLED shows a maximum luminance of 81156 cd/m^2. Moreover, by manipulating the excitons distribution, a WOLED can achieve a high color rendering index of 80. The findings may provide a new opportunity to achieve high-efficiency, high-luminance and low efficiency roll-off WOLEDs.
 [DOI: 10.1149/2.0081806jss]

Manuscript submitted March 21, 2018; revised manuscript received May 1, 2018. Published June 15, 2018.

As about 25% of the global electricity is consumed for lightings, causing 1.9 GT of CO_2 emissions, organic light-emitting diodes (OLEDs) are being actively studied to reduce the energy demand because of their outstanding characteristics, such as high efficiency, low power consumption and flexibility.[1–5] To date, based on the adopted emitters, four types of white OLEDs (WOLEDs) have been reported, such as fluorescent WOLEDs, thermally activated delayed fluorescent (TADF) WOLEDs, fluorescent/phosphorescent hybrid WOLEDs and phosphorescent WOLEDs.[6–8] In the case of fluorescent WOLEDs, their efficiencies are very low (i.e., <30 lm/W) due to the nonradiative triplet excitons. On the other hand, TADF WOLEDs, hybrid WOLEDs and phosphorescent WOLEDs can theoretically achieve 100% internal quantum efficiency (IQE), since TADF and phosphorescent materials can harvest both singlet and triplet excitons.[9–11] Therefore, the last three kinds of WOLEDs have greater potential to the commercialization. However, the development of TADF WOLEDs is still in its infancy stage, since they usually exhibit low luminance and serious efficiency roll-off.[12–14] Thus, the efficiency at the practical luminance level (e.g., 1000 cd/m^2) is not high enough. For hybrid WOLEDs, i) if the triplet energy (T_1) of blue fluorophors is lower than that of phosphors, the introduction of interlayers between fluorescent and phosphorescent emitting layers (EMLs) is required, which undoubtedly increases the complexity, and such hybrid WOLEDs fail to achieve 100% IQE;[15–17] ii) if the T_1 of blue fluorophors is higher than that of phosphors, although the structures can be simple, it is difficult to synthesize such blue fluorophors.[18–20] Therefore, the full utilization of phosphors can be an alternative strategy to obtain high-efficiency phosphorescent WOLEDs.[21–23]

Generally, mixing two complementary colors (i.e., blue/orange and blue/red) or three primary colors (blue/green/red) are two ways to generate white emissions. Compared with three-color WOLEDs, two-color WOLEDs show simpler characteristics, such as short fabrication process and simplified device engineering. However, since only two emitters are adopted, the color rendering index (CRI) of two-color WOLEDs is usually low, which cannot satisfy the demand of most of lighting applications.[24–26] Thus, although structures of three-color WOLEDs are more complicated, high CRI can be obtained by adjusting the light emission intensity of each emitter, which is more favorable to the real-life industrialization.[27–29] However, the investigation of three-color WOLEDs lags behind that of two-color WOLEDs, indicating urgent efforts are required to study the effect of three-color WOLEDs. Besides, there are still only a few high-efficiency three-color WOLEDs in the literature.

In order to boost the efficiency, the thoughtful design and understanding of the EML may be the room for further enhancing the performance of three-color WOLEDs. As a matter of fact, there are some representative reported three-color WOLEDs. For example, Zhang et al. fabricated a three-color single-EML WOLED, achieving a maximum forward-viewing power efficiency (PE) of 33.7 lm/W and 14.4 lm/W at 1000 cd/m^2.[30] Ma et al. doped three different color guests in the same host mCP to form a three-color WOLED, obtaining a maximum forward-viewing PE of 41.3 lm/W.[31] They also used a hybrid structure combined with p-i-n doping techniques to establish a three-color WOLED, yielding a maximum forward-viewing PE of 41.7 lm/W.[32] Li et al. used a yellow delayed fluorescent material with adjustable color coordinates to organize a three-color WOLED, producing a maximum PE of 28.9 lm/W.[33] Previously, we also developed a series of three-color WOLEDs by dint of rational emitter selection and device structure.[34–38] However, despite some high-performance three-color WOLEDs have been reported, there are still some problems to be solved: i) the maximum efficiency of three-color WOLEDs is not high enough (e.g., only very few devices can exhibit the maximum forward-viewing PE ≥50.0 lm/W), indicating that excitons are not effectively manipulated; ii) the efficiency at high luminance is low (e.g., the forward-viewing efficiency is often < 30 lm/W at 1000 cd/m^2), limiting the practical applications.

In this paper, for the first time, double blue EMLs have been functioned as the main exciton generation zone to achieve high-performance three-color phosphorescent WOLEDs. By dint of the new exciton-harvesting structure, the three-color WOLED can exhibit the maximum forward-viewing external quantum efficiency (EQE) and PE of 21.2% and 50.0 lm/W, respectively. Even at the illumination-relevant luminance of 1000 cd/m^2, the forward-viewing EQE and PE are as high as 18.0% and 32.5 lm/W, respectively, indicating very low efficiency roll-off. Besides, the WOLED shows a maximum luminance of 81156 cd/m^2. To the best of our knowledge, the maximum efficiencies, the efficiencies at 1000 cd/m^2 and the maximum luminance are among the best WOLEDs. Moreover, by manipulating the excitons distribution, a WOLED can achieve a CRI as high as 80, meeting the requirement of indoor lighting.

[z]E-mail: lyd66@163.com; l.baiquan@mail.scut.edu.cn

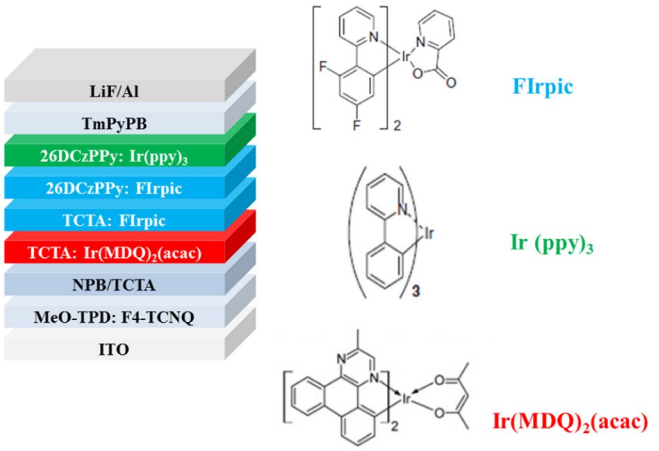

Figure 1. Schematic device structures of the three-color WOLED and the chemical structure of emitters.

Results and Discussion

Device structures and fabrication.—As shown in Fig. 1, the WOLED (W1) has the configuration of ITO/ MeO-TPD: F4-TCNQ (100 nm, 1: 4%)/ NPB (15 nm)/ TCTA(5 nm)/ TCTA: $Ir(MDQ)_2(acac)$ (5 nm, 1: 10%)/ TCTA: FIrpic (2 nm, 1: 7%)/ 26DCzPPy: FIrpic (4 nm, 1: 20%)/ 26DCzPPy: $Ir(ppy)_3$ (1 nm, 1: 6%)/ TmPyPB (50 nm)/ LiF(1 nm)/ Al (200 nm), where ITO is indium tin oxide, MeO-TPD is N, N, N',N'- tetrakis(4-methoxyphenyl)-benzidine, F4-TCNQ is tetrafluoro-tetracyanoqino dimethane, NPB is N,N'-di(naphthalene-1-yl)-N,N'-diph enyl-benzidine, TCTA is 4,4',4''-tri(9-carbazoyl) triphenylamine, $Ir(MDQ)_2(acac)$ is Iridium(III)bis(2-methyldi-benzo-[f,h]quinoxaline)(acetylacetonate), FIrpic is iridiu m(III)bis[(4,6-difluo-rophenyl)-pyridinato-N,C2 is 26DCzPPy is 2,6-bis(3-(carbazol-9-yl)phenyl)pyridine, $Ir(ppy)_3$ is tris(2-phenylpyridinne)iridium(III), TmPyPB (1,3,5-tri(m-pyrid-3-yl-phenyl)benzene and the the doping percentage is controlled by the thickness. All materials were commercially bought. Without breaking the vacuum, all material layers were thermally deposited at a base pressure of 2×10^{-7} Torr. For the doping layers, deposition rates of host and guest were controlled by their correspondingly independent quartz crystal oscillators. After preparation under a nitrogen atmosphere using epoxy glue and glass lids, all devices were encapsulated immediately. The Commission International de I'Eclairage (CIE) coordinates, correlated color temperature (CCT), CRI and electroluminescent (EL) spectra were recorded via a Konica Minolta CS2000 spectra system. The emission area of all devices is 3×3 mm^2 as defined by the overlapping area of the anode and cathode. By utilizing a computer-controlled source meter (Keithley 2400) and multimeter (Keithley 2000) with a calibrated silicon photodiode, the current density (J)-voltage (V)-luminance properties were recorded simultaneously.

Device design strategy.—To guarantee that high-performance three-color WOLEDs can be developed, we have adopted several strategies. First, a novel exciton-harvesting structure is designed by using the double blue EMLs instead of a single blue EML as the main exciton generation zone (i.e., TCTA: FIrpic/ 26DCzPPy: FIrpic), which is unlike previous reports. For example, the yellow EMLs are sandwiched by blue EMLs in Su's two-color WOLED,[39] while only single blue EML is used in Leo's device.[21] Besides, although the double-EML structure has been demonstrated to effectively enhance the performance of monochromatic OLEDs,[40–42] it has not yet been used to develop three-color WOLEDs so far. By dint of the double blue EMLs, the exciton generation zone can be greatly broadened, reducing the efficiency roll-off. As a result, high efficiency at high luminance can be achieved. Meanwhile, the double blue EMLs are sandwiched by red and green EMLs (contrast to Su's device[39]), which can harvest the excitons that are not consumed by blue EMLs, maximizing the exciton use efficiency.

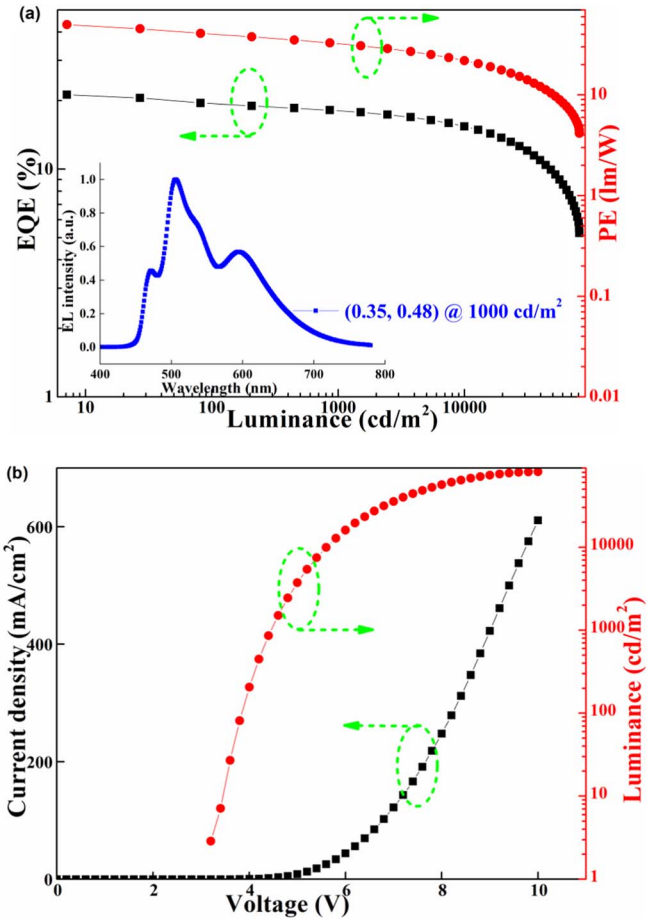

Figure 2. (a) Forward-viewing EQE and PE of W1 as a function of luminance. Inset: the EL spectrum at 1000 cd/m^2. (b) Current density and luminance of W1 as a function of voltage.

Performance of the three-color WOLED.—Based on the above considerations, high-performance three-color WOLEDs can be expected. As displayed in Fig. 2a, the maximum forward-viewing EQE and PE of W1 are 21.2% and 50.0 lm/W, respectively. At the display-relevant luminance of 100 cd/m^2, the forward-viewing EQE and PE are 19.4% and 40.9 lm/W, respectively. Even at the illumination-relevant luminance of 1000 cd/m^2, the forward-viewing EQE and PE are as high as 18.0% and 32.5 lm/W, respectively, indicating very low efficiency roll-off.[1–15] Since illumination sources have been generally represented by the total emitted power,[15] the maximum total PE of W1 is 85 lm/W, which only slightly decreased to 69.5 lm W^{-1} at the practical luminance of 1000 cd/m^2. In fact, the efficiency has almost overtaken the fluorescent lamps (with typical PE of 40-70 lm/W) at 1000 cd/m^2, demonstrating the advantage of our novel WOLED.

In addition, the CIE coordinates of W1 is (0.35, 0.48) at 1000 cd/m^2, which well locates within the white color region.[1–5] The CRI is 67, which is higher than that of representative three-color WOLEDs.[30] Besides, according to Gnade's report, the CRI>60 is acceptable for applications.[43] Therefore, it is easily seen that our WOLED is promising for the practical use. Furthermore, the CCT is 5125 K, which is close to that of sunlight at noon.[34] As shown in Fig. 2b, the turn-on voltage is 3.2 V (>1 cd/m^2), and the voltage is 3.85 and 4.45 V at 100 and 1000 cd/m^2, respectively, which are among the low-

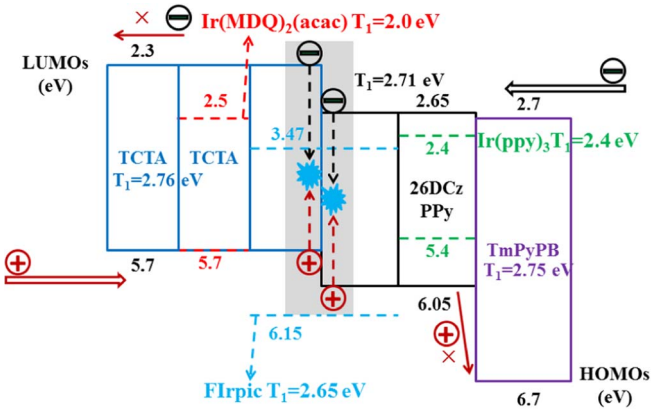

Figure 3. The charge/exciton confining structure for device W1 and the schematic diagram of EL procedures. The gray filled rectangle is the main exciton generation zone.

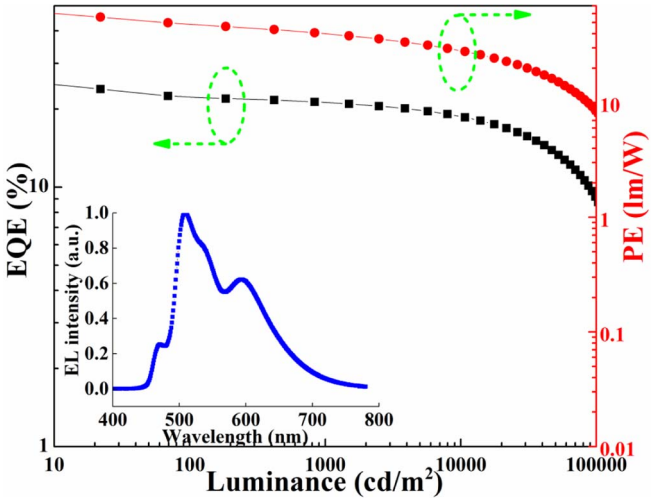

Figure 4. Forward-viewing EQE and PE of W2 as a function of luminance. Inset: the EL spectrum at 1000 cd/m^2.

est three-color phosphorescent WOLEDs. Remarkably, the maximum luminance is 81156 cd/m^2, which is among the highest WOLEDs.

Origin of the high performance.—*The working mechanism of three-color WOLEDs.*—Galvanized by the superior properties obtained from the novel WOLED, we then make a comprehensive investigation in order to reveal the origin of high performance. First, to effectively manage the excitons, suitable hosts have been employed. As shown in Fig. 3, 26DCzPPy is selected, because: i) the T_1 is 2.71 eV, satisfying FIrpic (2.65 eV) and Ir(ppy)$_3$ (2.4 eV),[24] which cannot only prevent the reverse energy transfer from FIrpic/ Ir(ppy)$_3$ to 26DCzPPy but also confine triplets in the whole EML, effectively enhancing the efficiency; ii) the similar hole and electron mobility [$\sim 10^{-5}$ cm^2/(V s)] can broaden the excitons recombination zone and achieve balanced charges transport for the recombination procedure, leading to the high efficiency and low efficiency roll-off.[24] iii) the lowest unoccupied molecular orbital (LUMO) and highest occupied molecular orbital (HOMO) of 26DCzPPy are 2.65 eV and 6.05 eV, respectively, well matching with those of nearby layers to diminish the charge transport barrier, which can lower the driving voltages and further boost the efficiency. TCTA is chosen, since i) its T_1 (2.76 eV) is higher than that of Firpic and Ir(MDQ)$_2$(acac) (2.0 eV),[27] prohibiting the reverse energy transfer; ii) it also functioned as the hole transport layer (HTL), which can reduce the heterojunction between HTL and EML, enhancing the performance.[3]

Next, the utilization of charges/excitons confining structure has a substantial influence on ensuring the performance. NPB/TCTA is selected as the stepwise HTL, which cannot only give an effective hole injection due to the matched HOMOs, but also effectively confine excitons/electrons in the EML because of the high T_1 and p-type property of TCTA.[27] On the other hand, TmPyPB is chosen as the electron transport layer (ETL) because of: i) its high electron mobility [10^{-3} cm^2/(V s)],[24] resulting in an enhanced charge balance due to the effective electron injection; ii) a higher T_1 (2.75 eV) than the host and guests in the nearby EML, confining triplets. iii) a deep HOMO of 6.7 eV, the big difference in HOMO levels (0.55 eV) between TmPyPB and the guest FIrpic (or 0.65 eV between TmPyPB and 26DCzPPy), reducing the hole leakage. Therefore, both charges and excitons can be well confined within the EML via this excellent confining structure, enhancing the efficiency and reducing the efficiency roll-off.

Then, since blue (FIrpic), green (Ir(ppy)$_3$) and red (Ir(MDQ)$_2$(acac)) emitters are phosphorescent materials, both singlet and triplet excitons can be harnessed for emission. Additionally, the total thcikness of the four EMLs is as thin as 12 nm, which can lower the voltage, improving the efficiency.[6]

Finally, the novel exciton-harvesting EML structure is significant to the high performance. Due to the existed energy barriers coupled with the fact that TCTA is a p-type material and 26DCzPPy exhibits high electron mobility,[6] it can be easily inferred that the main exciton generation zone is located at the TCTA/26DCzPPy interface, which is effectively broadened via the double blue EML, reducing the triplet-triplet annihilation and efficiency roll-off.[3] In turn, the reduction in triplet-triplet annihilation can effectively enhance the efficiency.[3] For the excitons (singlets and triplets with a ratio of 1: 3) in the main exciton generation zone, they are firstly harvested by FIrpic to furnish the blue emission. For the unused excitons, they will be harvested by the surrounded red and green EMLs, since the energy levels of Ir(ppy)$_3$ and (Ir(MDQ)$_2$(acac) are lower than those of FIrpic. As a result, the red and green emission occurred from the combined effects of efficient energy transfer from FIrpic and exciton formation by direct charge trapping on Ir(ppy)$_3$ and (Ir(MDQ)$_2$(acac).[6] Therefore, a white emission is obtained from the above EL process, as illustrated in Fig. 3.

Energy transfer between EMLs.—To further understand the emission mechanism of W1, the energy transfer between EMLs is studied. As shown in Fig. 2a inset, the green emission intensity is the strongest, although only 1 nm green EML is used. On the other hand, despite the thickness of red EML is 5 times thicker than that of green EML, the red intensity is much lower than green intensity and only slightly stronger than the blue intensity. Therefore, these facts suggest that the green EML plays a vital role in the performance, which can be explained as follows. Although the main exciton generation zone is located at the TCTA/26DCzPPy interface, holes can still be easily transported to the green EML due to the bipolar property of 26DczPPy, and meet electrons to form excitons, which can be harvested by Ir(ppy)$_3$ to enhance the green emission. However, due to the unipolar characteristic of TCTA, electrons are relatively difficult to reach the red EML. Hence, the direct exciton formation on Ir(MDQ)$_2$(acac) is inefficient, and the red emission is mainly originated from the energy transfer from FIrpic. For the green EML, both direct exciton formation on Ir(ppy)$_3$ and the energy transfer from FIrpic are very effective, leading to the strong green intensity.

To further clarify the effect of green EML, a thicker green EML (3 nm) has been used to fabricate device W2. To keep the total thickness of EMLs to be constant, the blue EML 26DCzPPy: FIrpic has been decreased to 2 nm. As a result, the EML structure of W2 is TCTA: Ir(MDQ)$_2$(acac) (5 nm,10%)/ TCTA: FIrpic (2 nm,7%)/ 26DCzPPy: FIrpic (2 nm, 20%)/ 26DCzPPy: Ir(ppy)$_3$ (3 nm, 6%), where other layers of W2 is the same as those of W1. As shown in Fig. 4 inset, the green intensity of W2 has been further intensified while the blue intensity has been weakened compared with W1. This is because more excitons are harvested by Ir(ppy)$_3$ due to the increased thickness of

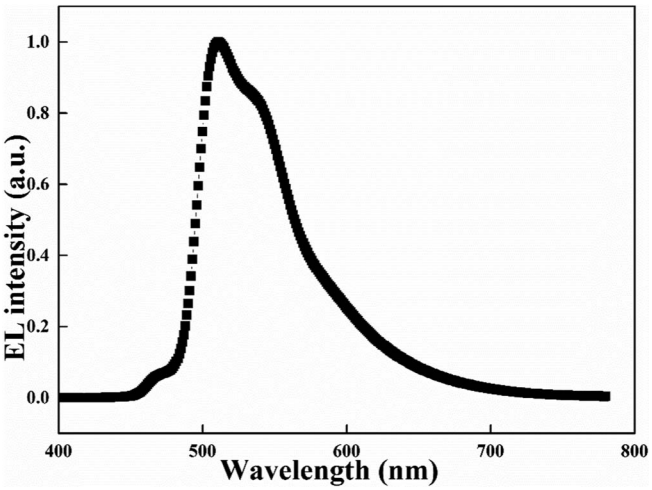

Figure 5. The EL spectrum of W3 at 1000 cd/m^2.

green EML.[6] Besides, since Ir(ppy)$_3$ is more efficient than FIrpic and Ir(MDQ)$_2$(acac), the increased green intensity renders the fact that the efficiency of W2 is higher than that of W1. For example, the forward-viewing PE at 1000 cd/m^2 is 40.2 lm/W, which is 24% higher than that of W1. However, the CIE coordinates of W2 is (0.37, 0.51), which is somewhat greenish due to the intensified green emission. Therefore, these facts not only suggest that the device performance is very sensitive to the green EML, but also imply that how to manipulate the excitons distribution is a key factor to guarantee the high-performance three-color WOLEDs.

Effects of host in green EML.—Since the green EML has a great influence on the performance, the effect of host in green EML has been investigated. By replacing 26DCzPPy with GH054 (bought from Nichem company), device W3 has been fabricated. Hence, the green EML structure of W3 is GH054: Ir(ppy)$_3$ (1 nm, 6%), where other layers of W3 is the same as those of W1. As shown in Fig. 5, only strong green emission can be observed with the CIE coordinates of (0.31, 0.60), while both blue and red emissions are almost disappeared, leading to no white emission. This phenomenon can be explained as follows. Although the T_1 of GH054 is higher than that of Ir(ppy)$_3$, it is lower than that of 26DCzPPy and FIrpic,[44] resulting in the fact that high-energy excitons in the double blue EMLs are easily transferred to the green EML. Besides, since most of excitons are transferred to the green EML, almost no excitons can be harvested by Ir(MDQ)$_2$(acac) from the energy transfer, further demonstrating the above analysis that the red emission in W1 is mainly originated from the energy transfer from FIrpic. Therefore, although the green EML is as thin as 1 nm, the host in green EML can vastly manipulate the excitons distribution, which is significant to the performance.

High-CRI WOLEDs.—Based on the above analyses, by manipulating the excitons distribution, the device performance can be regulated. Thus, high CRIs may be expected, if more balanced blue, green and red emission can be achieved.[45] Towards this end, the green emission should be decreased, while the blue and/or red intensity should be enhanced. Since excitons are easily harvested by Ir(ppy)$_3$ in our exciton-confining structure, a thinner green EML is required for the balanced emission. Therefore, the thickness of green EML has been decreased to 0.3 nm in device W4, which can render more excitons to be harnessed by blue and red EMLs, improving the blue and red emission. On the other hand, the thickness of red EML has been increased to 5.7 nm, which keeps the total thickness of EMLs to be same as that of W1. Meanwhile, due to the increased red EML, more excitons can be harvested by Ir(MDQ)$_2$(acac), further enhancing the red emission.[46–48] The EML structure of W4 is TCTA: Ir(MDQ)$_2$(acac) (5.7 nm,10%)/ TCTA: FIrpic (2 nm,7%)/ 26DCzPPy: FIrpic (4 nm, 20%)/ 26DCzPPy: Ir(ppy)$_3$ (0.3 nm, 6%), where other layers of W4 is the same as those of W1. As expected, more balanced emission is achieved in W4 (Fig. 6a inset). Remarkably, a high CRI of 80 is achieved, which can meet the requirement of indoor lighting (CRI ≥80),[1–5] demonstrating the successful manipulation of excitons distribution. Besides, since FIrpic is a sky-blue emitter (~472 nm), it is challenging for FIrpic-based three-color WOLEDs to show high CRI ≥80,[49] which further indicates the advantage of our novel exciton-harvesting structure. The CIE coordinates is (0.43, 0.42) with a CCT of 3235 K, locating the warm-white region. However, the efficiency of W4 is not as high as that of W1. For instance, the forward-viewing EQE and PE are 11.4% and 15.0 lm/W at 1000 cd/m^2, respectively, lower than those of W1. These phenomena can be attributed to the reduced green emission and greatly enhanced red emission, since Ir(MDQ)$_2$(acac) is much less efficient than Ir(ppy)$_3$. However, it is deserved to point out that the efficiency of W4 can be high enough, if more efficient red emitter can be obtained.

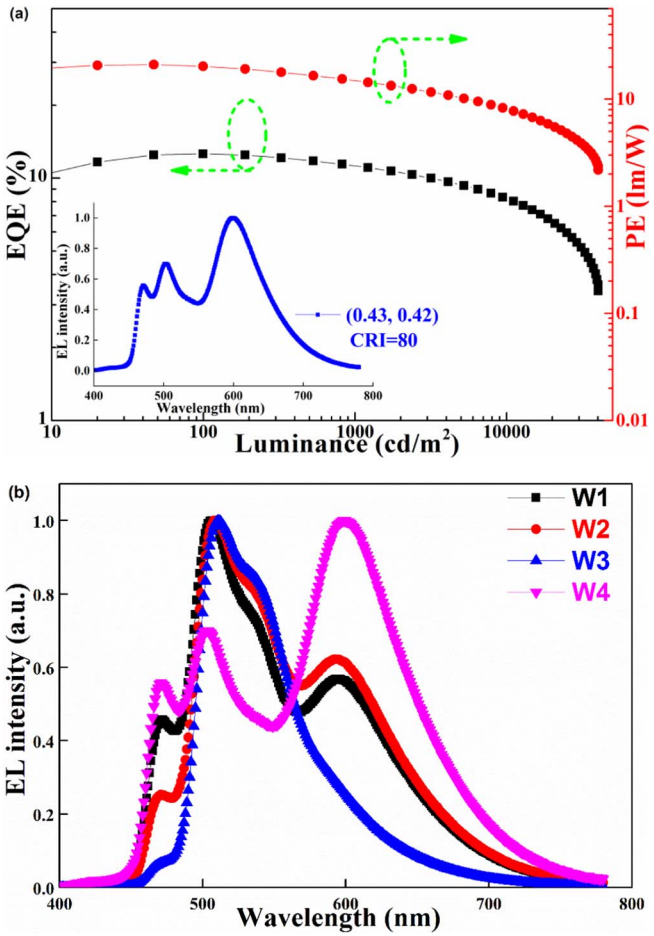

Figure 6. (a) Forward-viewing EQE and PE of W4 as a function of luminance. Inset: the EL spectrum at 1000 cd/m^2. (b) The comparison for the spectra of W1, W2, W3 and W4.

Conclusions

In summary, double blue EMLs, for the first time, have been functioned as the main exciton generation zone to obtain high-performance three-color phosphorescent WOLEDs. The WOLED can exhibit the maximum forward-viewing EQE and PE of 21.2% and 50.0 lm/W, respectively. Even at 1000 cd/m^2, the forward-viewing EQE and PE are as high as 18.0% and 32.5 lm/W, respectively, indicating very low efficiency roll-off. Besides, a maximum luminance of 81156 cd/m^2 is obtained. To our knowledge, these values are among the state-of-the-

art WOLEDs. Moreover, by manipulating the excitons distribution, a WOLED can achieve a high CRI of 80. Such results may provide a new opportunity to achieve high-efficiency, high-luminance and low efficiency roll-off WOLEDs, which will be beneficial to the design of both material and device structure for high-performance WOLEDs.

Acknowledgments

This research is supported by Project supported by the National Key Research Program "National Quality Based Common Technology Research and Application" Key Projects (2016YFF0203600), National Quality Public Welfare Special Plan (201510077-02), Science and Technology Plan of Administration of Quality and Technology Supervision of Guangdong Province (2016CZ01), National key research and development program (2016YFF0203603), Tiptop Scientific and Technical Innovative Youth Talents of Guangdong Special Support Program (2015TQ01C777, 2016TQ03C331), Pearl Rive S&T Nova Program of Guangzhou (201806010090,201710010066, 201610010052).

ORCID

Baiquan Liu https://orcid.org/0000-0001-5761-9654

References

1. X. Yang, G. Zhou, and W. Y. Wong, *Chem. Soc. Rev.*, **44**, 8484 (2015).
2. C. Fan and C. Yang, *Chem. Soc. Rev.*, **43**, 6439 (2014).
3. Q. Wang and D. Ma, *Chem. Soc. Rev.*, **39**, 2387 (2010).
4. H. Sasabe and J. Kido, *J. Mater. Chem. C*, **1**, 1699 (2013).
5. M. C. Gather, A. Kohenen, and K. Meerholz, *Adv. Mater.*, **23** 233 (2011).
6. B. Q. Liu, X. Li, H. Tao, J. H. Zou, M. Xu, L. Wang, J. B. Peng, and Y. Cao, *J. Mater. Chem. C*, **5**, 7668 (2017).
7. J. Chen, F. Zhao, and D. Ma, *Mater. Today*, **17**, 175 (2014).
8. D. Zhang, L. Duan, Y. Zhang, M. Cai, D. Zhang, and Y. Qiu, *Light: Sci. Appl.*, **4**, e232 (2016).
9. C. J. Chiang, A. Kimyonok, M. K. Etherington, G. C. Griffiths, V. Jankus, F. Turksoy, and A. P. Monkman, *Adv. Funct. Mater.*, **23**, 739 (2013).
10. G. Schwartz, S. Reineke, T. Rosenow, K. Walzer, and K. Leo, *Adv. Funct. Mater.*, **19**, 1319 (2009).
11. L. Zhou, Q. D. Ou, Y. Q. Li, H. Y. Xiang, L. H. Xu, J. D. Chen, C. Li, S. Shen, S. T. Lee, and J. X. Tang, *Adv. Funct. Mater.*, **25**, 2660 (2015).
12. T. Higuchi, H. Nakanotani, and C. Adachi, *Adv. Mater.*, **27**, 2019 (2015).
13. K. Song and J. Y. Lee, *Adv. Mater.*, **27**, 4358 (2015).
14. H. Uoyama, K. Goushi, K. Shizu, H. Nomura, and C. Adachi, *Nature*, **492**, 234 (2012).
15. Y. Sun, N. Giebink, H. Kanno, B. Ma, M. Thompson, and S. R. Forrest, *Nature*, **440**, 908 (2006).
16. P. Chen, W. Xie, J. Li, T. Guan, Y. Duan, Y. Zhao, S. Liu, C. Ma, L. Zhang, and B. Li, *Appl. Phys. Lett.*, **91**, 023505 (2007).
17. B. Liu, L. Wang, M. Xu, H. Tao, J. Zou, D. Gao, L. Lan, H. Ning, J. Peng, and Y. Cao, *Sci. Rep.*, **4**, 7198 (2014).
18. B. Liu, L. Wang, D. Gao, J. Zou, H. Ning, J. Peng, and Y. Cao, *Light: Sci. Appl.*, **5**, e16137 (2016).
19. J. Ye, C. J. Zheng, X. M. Ou, X. H. Zhang, M. K. Fung, and C. S. Lee, *Adv. Mater.*, **24**, 3410 (2012).
20. D. Zhang, L. Duan, Y. Li, D. Zhang, and Y. Qiu, *J. Mater. Chem. C*, **2**, 8191 (2014)
21. S. Reineke, F. Lindner1, G. Schwartz, N. Seidler, K. Walzer, B. Lussem, and K. Leo, *Nature*, **14**, 234 (2009).
22. Q. D. Ou, L. Zhou, Y. Q. Li, S. Chen, J. D. Chen, C. Li, Q. K. Wang, S. T. Lee, and J. X. Tang, *Adv. Funct. Mater.*, **24**, 7249 (2014).
23. B. Zhang, G. Tan, C. S. Lam, B. Yao, C. L. Ho, L. Liu, Z. Xie, W. Y. Wong, J. Ding, and L. Wang, *Adv. Mater.*, **24**, 1873 (2012).
24. B. Liu, L. Wang, D. Gao, M. Xu, X. Zhu, J. Zou, L. Lan, H. Ning, J. Peng, and Y. Cao, *Mater. Horiz.*, **2**, 536 (2015).
25. Q. Wang, I. W. H. Oswald, M. R. Perez, H. Jia, A. A. Shahub, Q. Qiao, B. E. Gnade, and M. A. Omary, *Adv. Funct. Mater.*, **24**, 4746 (2014).
26. S. Lee, H. Shin, and J. J. Kim, *Adv. Mater.*, **26**, 5864 (2014).
27. F. Zhao, Z. Zhang, Y. Liu, Y. Dai, J. Chen, and D. Ma, *Org. Electron.*, **13**, 1049 (2012).
28. L. J. Zhang, Y. L. Hua, X. M. Wu, Y. Wang, and S. G. Yin, *Chin. Phys. B*, **17**, 3097 (2008).
29. J. Yu, H. Lin, F. Wang, Y. Lin, J. Zhang, H. Zhang, Z. Wang, and B. Wei, *J. Chem. Mater.*, **22**, 22097 (2012).
30. C. J. Zheng, J. Wang, J. Ye, M. F. Lo, X. K. Liu, M. K. Fung, X. H. Zhang, and C. S. Lee, *Adv. Mater.*, **25**, 2205 (2013).
31. Q. Wang, J. Ding, D. Ma, Y. Cheng, L. Wang, and F. Wang, *Adv. Mater.*, **21**, 2397 (2009).
32. N. Sun, Q. Wang, Y. Zhao, Y. Chen, D. Yang, F. Zhao, J. Chen, and D. Ma, *Adv. Mater.*, **26**, 1617 (2014).
33. X. L. Li, G. Xie, M. Liu, D. Chen, X. Cai, J. Peng, Y. Cao, and S. J. Su, *Adv. Mater.*, **28**, 4614 (2016).
34. B. Liu, H. Nie, X. Zhou, S. Hu, D. Luo, D. Gao, J. Zou, M. Xu, L. Wang, Z. Zhao, A. Qin, J. Peng, H. Ning, Y. Cao, and B. Z. Tang, *Adv. Funct. Mater.*, **26**, 776 (2016).
35. B. Liu, H. Tao, L. Wang, D. Gao, W. Liu, J. Zou, M. Xu, H. Ning, J. Peng, and Y. Cao, *Nano Energy*, **26**, 26 (2016).
36. B. Liu, M. Xu, L. Wang, H. Tao, Y. Su, D. Gao, L. Lan, J. Zou, and J. Peng, *Nano-Micro Lett.*, **6**, 335 (2014).
37. B. Q. Liu, M. Xu, L. Wang, J. H. Zou, H. Tao, Y. J. Su, D. Y. Gao, H. L. Ning, L. F. Lan, and J. B. Peng, *Org. Electron.* **15**, 2616 (2014).
38. B. Liu, H. Nie, G. Lin, S. Hu, D. Gao, J. Zou, M. Xu, L. Wang, Z. Zhao, H. Ning, J. Peng, Y. Cao, and B. Z. Tang, *ACS Appl. Mater. Interfaces*, **9**, 34162 (2017).
39. S. J. Su, E. Gonmori, H. Sasabe, and J. Kido, *Adv. Mater.*, **20**, 4189 (2008).
40. X. Zhou, D. S. Qin, M. Pfeiffer, J. Blochwitz-Nimoth, A. Werner, J. Drechsel, B. Maennig, K. Leo, M. Bold, P. Erk, and H. Hartmann, *Appl. Phys. Lett.*, **81**, 4070 (2002).
41. G. He, M. Pfeiffer, K. Leo, M. Hofmann, J. Bimstock, R. Pudzich, and J. Salbeck, *Appl. Phys. Lett.*, **85**, 3911 (2004).
42. H. Sun, Q. Guo, D. Yang, Y. Chen, J. Chen, and D. Ma, *ACS Photonics*, **2**, 271 (2015).
43. U. S. Bhansali, H. Jia, I. W. Oswald, M. A. Omary, and B. E. Gnade, *Appl. Phys. Lett.*, **100**, 183305 (2012).
44. http://www.nichem.com.tw/s/2/about.html.
45. W. Ji, J. Zhao, Z. Sun, and W. Xie, *Org. Electron.*, **12**, 1137 (2011).
46. X. H. Zhao, Z. S. Zhang, Y. Qian, M. D. Yi, L. H. Xie, C. P. Hu, G. H. Xie, H. Xu, C. M. Han, Y. Zhao, and W. Huang, *J. Mater. Chem. C*, **1**, 3482 (2013).
47. K. Xue, G. Han, Y. Duan, P. Chen, Y. Yang, D. Yang, Y. Duan, X. Wang, and Y. Zhao, *Org. Electron.*, **18**, 84 (2015).
48. B. Liu, M. Xu, L. Wang, X. Yan, H. Tao, Y. Su, D. Gao, L. Lan, J. Zou, and J. Peng, *Org. Electron.*, **15**, 926 (2014).
49. Y. L. Chang, Y. Song, Z. Wang, M. G. Helander, J. Qiu, L. Chai, Z. Liu, G. D. Scholes, and Z. Lu, *Adv. Funct. Mater.*, **23**, 705 (2013).